Brassinosteroids Rescue the Deficiency of CYP90, a Cytochrome P450, Controlling Cell Elongation and De-etiolation in Arabidopsis

Miklós Szekeres,* Kinga Németh,[†]
Zsuzsanna Koncz-Kálmán,[†] Jaideep Mathur,[†]
Annette Kauschmann,[‡] Thomas Altmann,[‡]
George P. Rédei,[§] Ferenc Nagy,* Jeff Schell,[†]
and Csaba Koncz*[†]
*Institute of Plant Biology
Biological Research Center
Hungarian Academy of Sciences
H-6701 Szeged
Hungary
[†]Max-Planck-Institut für Züchtungsforschung
D-50829 Köln
Federal Republic of Germany
[‡]Max-Planck-Institut für Molekulare
Pflanzenphysiologie
D-14476 Golm
Federal Republic of Germany
[§]3005 Woodbine Court
Columbia, Missouri 65203-0906

Summary

The *cpd* mutation localized by T-DNA tagging on Arabidopsis chromosome 5-14.3 inhibits cell elongation controlled by the ecdysone-like brassinosteroid hormone brassinolide. The *cpd* mutant displays de-etiolation and derepression of light-induced genes in the dark, as well as dwarfism, male sterility, and activation of stress-regulated genes in the light. The *CPD* gene encodes a cytochrome P450 (CYP90) sharing homologous domains with steroid hydroxylases. The phenotype of the *cpd* mutant is restored to wild type both by feeding with C23-hydroxylated brassinolide precursors and by ectopic overexpression of the *CPD* cDNA. Brassinosteroids also compensate for different cell elongation defects of Arabidopsis *det*, *cop*, *fus*, and *axr2* mutants, indicating that these steroids play an essential role in the regulation of plant development.

Introduction

Cell elongation plays a crucial role in the early postembryonic development of higher plants. Water uptake into the dry embryo induces a rapid elongation of cells in the hypocotyl and reactivates cell division in the meristems. Light signals, activating the phytochrome or blue/ultraviolet photoreceptors (or both), induce photomorphogenesis and de-etiolation, resulting in the inhibition of hypocotyl elongation, opening of the apical hook of cotyledons, induction of greening, and elongation of leaf primordia. In the absence of light, the elongation of hypocotyl and root is not inhibited, and the apical hook of cotyledons is maintained. The dark pathway of seedling development is referred to as skotomorphogenesis because in the presence of suitable carbon and nitrogen sources plants are capable of heterotrophic growth and can complete their life cycle in the dark (for reviews see Deng, 1994; Kendrick and Kronenberg, 1994).

The exclusion of light signaling offers a relatively simple system for the genetic dissection of developmental and hormonal pathways controlling cell elongation in defined plant organs. Arabidopsis mutations causing de-etiolation (*det*; Chory and Susek, 1994), constitutive photomorphogenesis (*cop*; Deng, 1994), embryo and seedling lethality (*emb/fus*; Castle and Meinke, 1994; Miséra et al., 1994), constitutive ethylene response (*ctr1*; Ecker, 1995), and auxin resistance (*axr2*; Estelle and Klee, 1994) have been shown to result in a similar inhibition of hypocotyl elongation. Cell elongation abnormalities found in auxin and ethylene signaling mutants are consistent with physiological data, demonstrating the requirement for auxin and inhibition by ethylene of cell elongation in the hypocotyl (Davies, 1987). The *DET*, *COP*, and *FUS* genes are thought to code for specific negative regulators of light signaling because the developmental and molecular phenotypes of *det*, *cop*, and *fus* mutants are not altered by the *hy* mutations of photoreceptors (Quail et al., 1995). Nonetheless, because these mutations have severe pleiotropic effects, it is likely that the *DET*, *COP*, and *FUS* genes play a more general role in transcriptional regulation (Millar et al., 1994). In support of this notion, a *dim* mutation, inhibiting hypocotyl elongation without an apparent effect on light signaling, has been characterized and shown to affect the regulation of *TUB1* β-tubulin gene expression (Takahashi et al., 1995).

Here we describe an Arabidopsis cell elongation mutant, *cpd*, displaying skotomorphogenic developmental defects similar to those of *dim* and *det2* (Chory et al., 1991) mutants. The *cpd* mutation was isolated by T-DNA tagging and shown to abolish the synthesis of a cytochrome P450, CYP90, which shares homology with conserved domains of P450 monooxygenases, including steroid hydroxylases (Nelson et al., 1993). We demonstrate that the hypocotyl elongation defect of the *cpd* mutant can be rescued by C23-hydroxylated derivatives of cathasterone, a precursor of the ecdysone-like plant steroid hormone brassinolide (Mandava, 1988). Brassinosteroids (BRs) are also shown to overcome partially, or fully, the inhibition of hypocotyl elongation caused by the *det*, *cop*, *fus*, *dim*, and *axr2* mutations in Arabidopsis. The data indicate that CYP90 is involved in the biosynthesis of active BRs, which are essential for the regulation of cell elongation during plant development.

Results

Identification and Developmental Effects of the *cpd* Mutation
By screening for mutants defective in hypocotyl, root elongation, or both during skotomorphogenesis, a recessive mutation causing constitutive photomorphogenesis and dwarfism (*cpd*) was identified in an Arabidopsis T-DNA insertional mutant collection (Koncz et al.,
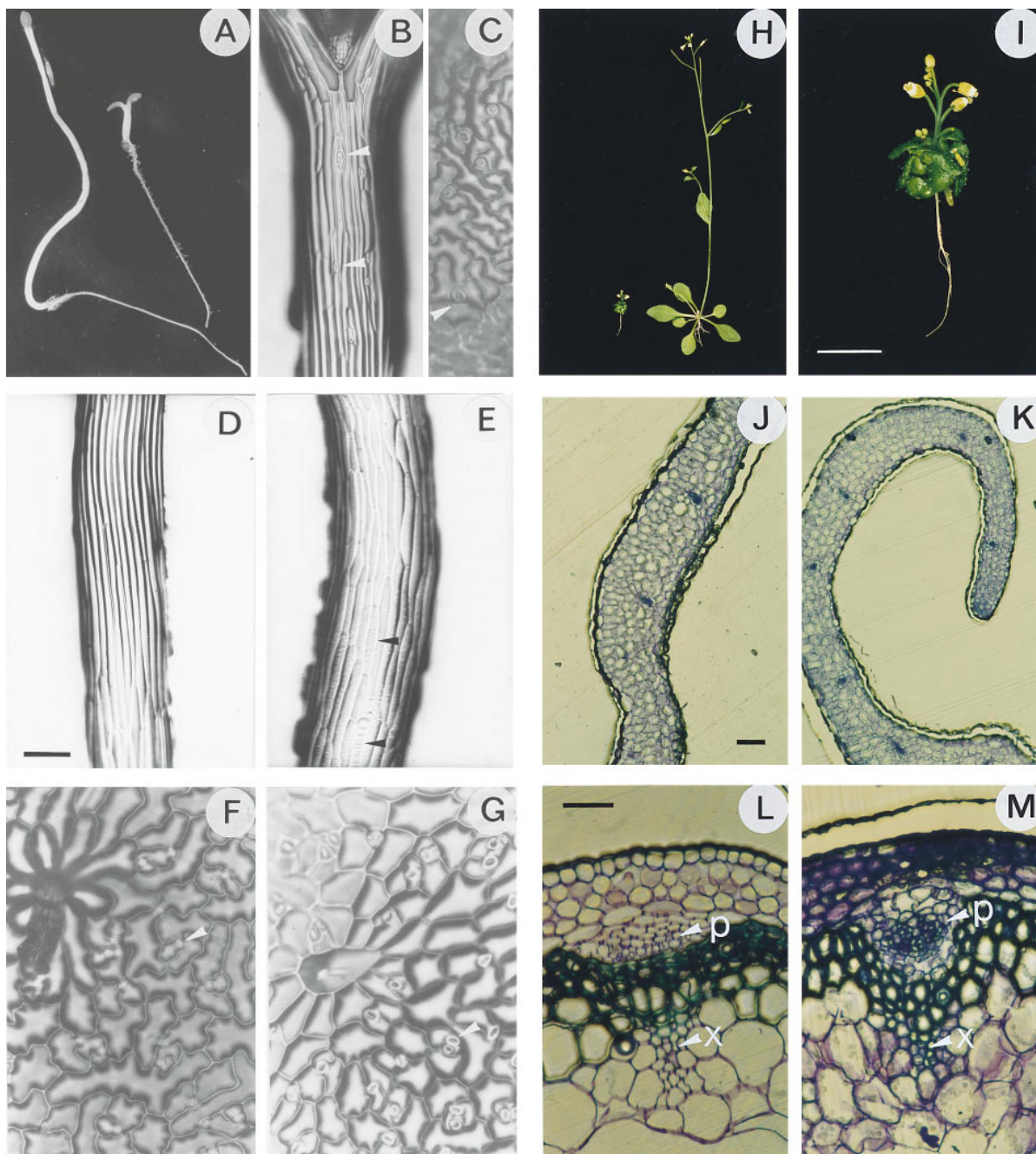
Figure 1. Effects of the *cpd* Mutation on Seedling Development in the Dark and Light

In the dark, the *cpd* mutant (right in [A]) exhibits short hypocotyl and open cotyledons, whereas the hypocotyl is elongated and the hook of cotyledons is closed in the wild type (left in [A]). Unusual cell division and guard cell differentiation in the hypocotyl epidermis (B) and closely spaced stomata in the cotyledon epidermis (C) are seen in the the *cpd* mutant. In contrast with wild type (D), the length of epidermal cells is reduced in the *cpd* mutant (E), and their surface is covered by transverse cellulose microfibrils (indicated by closed arrowheads). In comparison with wild type (F), the adaxial leaf epidermis of the *cpd* mutant (G) shows straight cell walls and duplicated stomatal structures. In the light (H), the *cpd* mutant (left) is smaller than the wild type (right), owing to inhibition of longitudinal growth in all organs (close-up of mutant in [I]). Cross sections of wild type (J) and *cpd* mutant (K) leaves show differences in the size and elongation of mesophyll cells. Comparison of the organization of phloem (p) and xylem (x) cell files in stem cross sections of wild-type (L) and *cpd* mutant (M) plants. (D) and (E), (F) and (G), (J) and (K), and (L) and (M) are identical magnifications. Scale bars represent 200 μm in (D) and 100 μm in (J) and (L).

1992b). Unlike the wild type, the *cpd* mutant developed a short hypocotyl, no apical hook, open cotyledons, and extended leaf primordia in the dark (Figures 1A and 1B). As compared with wild type, the length of epidermal cell files was reduced at least 5-fold in the hypocotyl, but decreased by only 20%–50% in the root of mutant seedlings. Epidermal cells of the mutant hypocotyl were decorated by thick transverse files of cellulose microfibrils
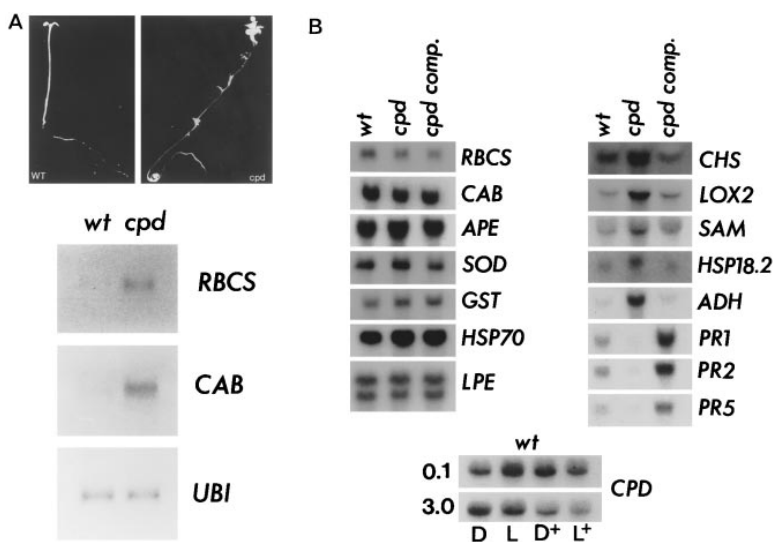
Figure 2. Altered Patterns of Gene Expression in the *cpd* Mutant and *CPD*-Overexpressing Plants in the Dark and Light

(A) Hybridization of RNAs prepared from wild-type (left) and *cpd* mutant (right) plants, grown in media with 15 mM sucrose for 5 weeks in the dark, with *RBCS*, *CAB*, and *UBI* gene probes.

(B) RNAs were prepared from wild-type (wt), *cpd* mutant (*cpd*), and genetically complemented *cpd* (*cpd* comp.) seedlings grown in glass jars under white light for 2 weeks and hybridized with the *RBCS*, *CAB*, alkaline peroxidase (*APE*), superoxide dismutase (*SOD*), gluthatione S-transferase (*GST*), *HSP70*, lignin-forming peroxidase (*LPE*), *CHS*, lipoxygenase (*LOX2*), S-adenosylmethionine synthase (*SAM*), *HSP18.2*, alcohol dehydrogenase (*ADH*), and pathogenesis-related *PR1*, *PR2*, and *PR5* gene probes. To control an equal loading of RNA samples, the blots were hybridized with the *UBI* gene probe (data not shown). The effects of light, cytokinin, and sucrose on the level of steady-state *CPD* RNA was assayed by transferring 10-day-old wild-type seedlings (grown in white light and in the presence of 15 mM sucrose) to media containing either 0.1% (3 mM) or 3% (90 mM) sucrose. These seedlings were further grown for 6 days in either dark (D) or light (L), with (D$^+$ and L$^+$) or without (D and L) cytokinin (1.5 μM 6[γ,γ-dimethylallylamino]-purine riboside) before RNA isolation.

(Figures 1D and 1E) and showed perpendicular divisions leading to differentiation of stomatal guard cells (Figure 1B). Dense stomata and trichomes characteristic for leaves were also observed on the epidermis of mutant cotyledons (Figure 1C). During growth for 5 weeks in the dark, the mutant developed numerous rosette leaves, while wild-type seedlings opened their cotyledons without leaf expansion under these conditions (Figure 2A). These phenotypic traits indicated a derepression of photomorphogenesis and de-etiolation in the dark-grown *cpd* mutant. Hybridization of steady-state RNAs prepared from these seedlings, using an ubiquitin (*UBI*) gene probe as an internal control, confirmed that morphological signs of de-etiolation in the mutant were accompanied by an increase in the expression of light-regulated genes coding for the small subunit of ribulose 1,5-bisphosphate carboxylase (RBCS) and the chlorophyll a/b-binding protein (CAB; Figure 2A).

When grown in soil under white light, the size of *cpd* mutant plants was 20- to 30-fold smaller than that of wild-type plants of the same age. Exposure to light induced greening and chloroplast differentiation in the periderm of mutant roots (data not shown) and resulted in a further inhibition of cell elongation, leading to an overall reduction of the length of petioles, leaves, inflorescence stems, and flower organs (Figures 1H and 1I). Histological analysis showed that in the round-shape epinastic mutant leaves the number of longitudinal mesophyll cell files was reduced and the palisade cells failed to elongate (Figures 1J and 1K). The cell walls were straightened in the adaxial leaf epidermis of the mutant, which displayed an amplification and duplication of stomatal guard cells (Figures 1F and 1G). Stem cross sections showed an unequal division of cambium, producing extranumerary phloem cell files at the expense of xylem cells in the mutant (Figures 1L and 1M). The *cpd* mutant was viable in soil and produced eggs

and pollen of wild-type size. However, the mutant did not set seeds because its pollen failed to elongate during germination, resulting in male sterility.

Genetic Analysis and Complementation of the *cpd* Mutation

After outcrossing of the mutant with wild type, the *cpd* mutation cosegregated with a single T-DNA insertion carrying a hygromycin resistance (*hpt*) marker gene from the Agrobacterium transformation vector pPCV5013Hyg (Koncz et al., 1989). The *cpd* mutation and the T-DNA insertion were mapped to chromosome 5-14.3 (Figure 3A) using trisomic testers and the *ttg* marker of chromosome 5 in repulsion (see Experimental Procedures).

The physical map of the T-DNA-tagged locus was determined by DNA hybridization and showed that the *cpd* mutant contained a T-DNA insert of 4.8 kb, which underwent internal rearrangements (Figure 3A). The T-DNA-tagged locus was isolated by constructing a genomic DNA library from the *cpd* mutant and mapped by hybridization with T-DNA-derived probes (Figure 3A). The T-DNA–plant DNA insert junctions were subcloned, sequenced, and used as probes to determine precisely the genomic location of the T-DNA insertion by isolation of Arabidopsis YAC (yeast artificial chromosome) clones. The YAC clones (Figure 3A) overlapped with the *ASA1* (anthranylate synthase, chromosome 5-14.7) and *hy5* (long hypocotyl locus, chromosome 5-14.8) region of chromosome 5 (R. Schmidt, unpublished data; Hauge et al., 1993), thus matching the map position (chromosome 5-14.3) determined for the T-DNA-tagged *cpd* mutation by genetic linkage analysis.

Plant DNA sequences flanking the *hpt*-pBR segment of T-DNA (Figure 3A) hybridized with an mRNA of 1.7 kb present in wild-type seedlings and cell suspension cultures, but failed to detect any transcript in the *cpd* mutant (Figure 3B). Using this probe, wild-type cDNA and genomic clones were isolated and characterized by
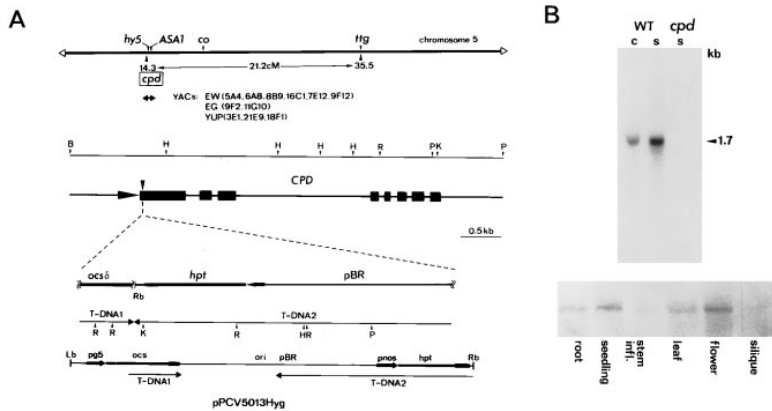
Figure 3. Chromosomal Localization, Physical Structure, and Transcription of Wild-Type and T-DNA-Tagged CPD Alleles

(A) Schematic genetic linkage map of Arabidopsis chromosome 5 (top line), showing the position of the T-DNA insertion and cpd mutation in relation to those of ttg (transparent testa glabra), co (constans), hy5 (long hypocotyl), and ASA1 (anthranylate synthase) loci. The second line shows the location of a YAC contig carrying the CPD gene. Schematic structure of the CPD gene and the position of the T-DNA insertion in the cpd allele are shown in the middle. The promoter of the CPD gene is labeled by an arrow, and exons are shown as thick black bars. The structure of the T-DNA insert is compared with that of the T-DNA of Agrobacterium transformation vector pPCV5013Hyg. The T-DNA insertion consists of two DNA segments (T-DNA1 and T-DNA2) carrying, respectively, part of the octopine synthase (ocs) gene and the hpt selectable marker gene in inverse orientation, as compared with the map of pPCV5013Hyg vector. Lines above the schematic map of the CPD gene and below the map of T-DNA insertion indicate restriction endonuclease cleavage sites. Abbreviations: ocs, octopine synthase gene; ocsδ, octopine synthase gene segment; hpt, hygromycin phosphotransferase gene; pBR, pBR322 plasmid replicon; ori, replication origin of pBR322; pg5, promoter of T-DNA gene 5; pnos, nopaline synthase promoter; Lb and Rb, respectively, left and right border sequences of the T-DNA; B, BamHI; H, HindIII; P, PstI; R, EcoRI; and K, KpnI.
(B) RNAs prepared from wild-type cell suspension culture (c), wild-type, and cpd mutant seedlings (s) were hybridized with the PstI–HindIII plant DNA–T-DNA junction fragment flanking the hpt-pBR segment (T-DNA2). RNAs prepared from seedlings and different organs of soil-grown plants were hybridized with the CPD cDNA as probe. stem infl., inflorescence stems.

nucleotide sequencing. In support of the RNA hybridization data, nucleotide sequence comparison of the T-DNA insert junctions with wild-type cDNA and genomic DNA sequences showed that the T-DNA was inserted 10 bp 3′-downstream of the ATG start codon of a gene, preventing the transcription of its coding region.

To demonstrate that the T-DNA insertion was indeed responsible for the cpd mutation, we cloned the coding region of wild-type cDNA in the plant gene expression vector pPCV701 and expressed it in the homozygous cpd mutant under the control of the auxin-regulated mannopine synthase (mas) 2′ promoter (Figure 4A) (Koncz et al., 1994). Transgenic plants, selected and regenerated with the aid of a kanamycin resistance gene carried by the pPCV701 vector, were all wild type and fertile, demonstrating genetic complementation of the cpd mutation. Kanamycin-resistant progeny of many complemented lines developed more expanded leaves and inflorescence branches than the wild type. One such complemented cpd line (Figure 4C) contained at least three independently segregating pPCV701 T-DNA insertions, since it yielded 268 kanamycin-resistant wild-type and 4 kanamycin-sensitive cpd mutant progeny. DNA fingerprinting confirmed the presence of multiple pPCV701 T-DNA insertions in this complemented line that produced a considerably higher amount of CPD transcript from the mas 2′ promoter–driven cDNA copies than the wild type from the single copy CPD gene (Figure 4B).

The cpd Mutation and CPD Overexpression Affect Stress-Regulated Gene Expression in the Light
In contrast with the dark-grown cpd mutant (see Figure 2A), in light-grown plants neither the absence nor the overexpression of CPD transcript affected the level of steady-state RNAs of light-regulated RBCS and CAB genes (see Figure 2B). The transcript levels of chalcone synthase (CHS), alcohol dehydrogenase (ADH), lipoxygenase (LOX2), S-adenosylmethionine synthase, and heat shock 18.2 (HSP18.2) genes were elevated in the cpd mutant, whereas the mRNA levels of other stress-regulated genes, such as alkaline peroxidase (APE), superoxide dismutase (SOD), glutathione S-transferase (GST), HSP70, or lignin-forming peroxidase (LPE), were comparable in the cpd mutant, wild-type, and CPD-overexpressing plants. The expression of the pathogenesis-related genes PR1, PR2, and PR5 was remarkably low in the cpd mutant. However, overexpression of the CPD cDNA resulted in a significant induction of these PR genes in the complemented lines.

The CPD Gene Encodes a Novel Cytochrome P450
DNA sequence analysis revealed that the CPD gene consists of eight exons (see Figure 3A) with consensus splice sites at the exon–intron boundaries. The CPD cDNA showed over 90% homology with expressed sequence tags (ESTs) (e.g., EMBL accession number Z29017 and GenBank accession number T43151) from several organ-specific Arabidopsis cDNA libraries, indicating that the CPD transcript is ubiquitous. Hybridization analysis with the cDNA probe (see Figure 3B) indeed showed that the levels of steady-state CPD mRNA were comparable in roots, leaves, and flowers, but considerably lower in inflorescence stems and green siliques (fruits). The expression of the CPD gene was found to be modulated by external signals, such as light, cytokinin growth factor, and sucrose provided as a carbon source. The levels of CPD mRNA were elevated in dark-grown wild-type seedlings either by increasing the sucrose content of the media (from 3 mM to 90 mM) or by exposure to light at low concentrations of sucrose, but decreased by combined cytokinin and sucrose treatments, particularly in the light (see Figure 2B).

Translation of the CPD cDNA defined a coding region of 472 codons for a protein of 53,785 Da. The deduced amino acid sequence of this protein detected homology
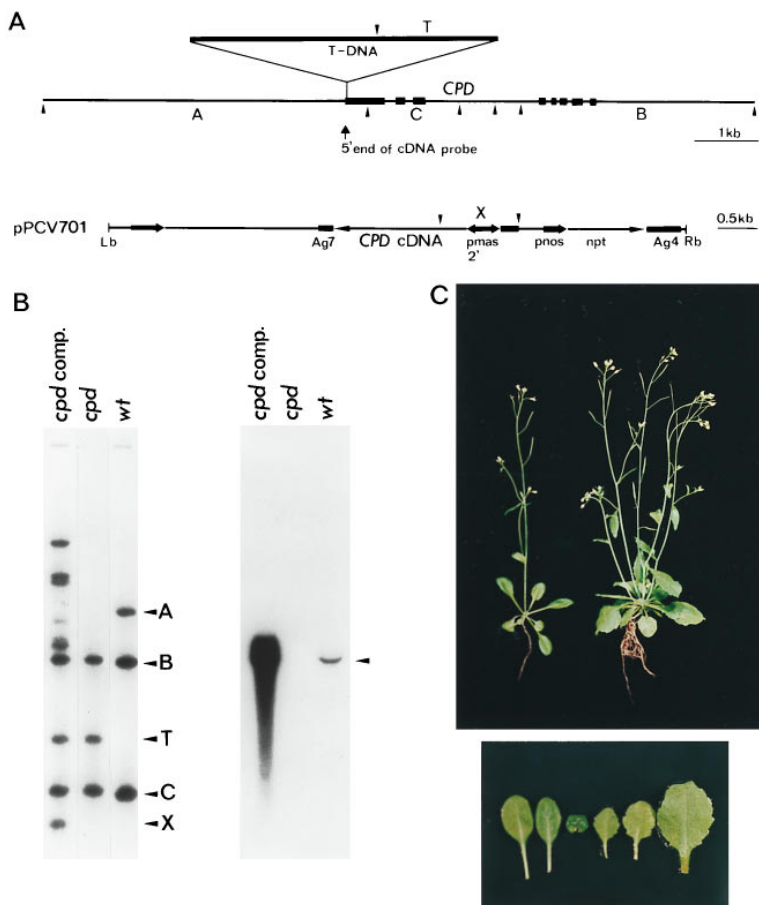
Figure 4. Genetic Complementation of the *cpd* Mutation

(A) Schematic maps of the T-DNA-tagged *cpd* gene and the T-DNA of plant gene expression vector pPCV701, carrying the *CPD* cDNA driven by the *mas* 2′ promoter. HindIII cleavage sites are indicated by closed arrowheads below the map of the *cpd* gene and above the map of pPCV701 expression vector. Fragments A, B, and C indicate HindIII fragments of the wild-type *CPD* gene hybridizing with the *CPD* cDNA probe. T labels the T-DNA–plant DNA junction fragment that hybridizes with the cDNA probe in the *cpd* mutant. X labels the HindIII fragment carrying the junction of the *mas* 2′ promoter and *CPD* cDNA. Because the 5′ end of the cDNA probe is located very close to the site of T-DNA insertion in the *cpd* gene, the cDNA probe did not detect the second T-DNA–plant DNA junction fragment, carrying part of the A fragment linked to the T-DNA. Abbreviations: Lb and Rb, respectively, left and right borders of the T-DNA of pPCV701 expression vector; pmas, promoter of the mannopine synthase gene; pnos, nopaline synthase promoter; npt, kanamycin resistance (neomycin phosphotransferase) gene; Ag7 and Ag4, respectively, polyadenylation sequences derived from T-DNA genes 4 and 7.

(B) Southern hybridization (left) of HindIII-digested DNAs from wild type, *cpd* mutant, and a *CPD*-overexpressing complemented line with the *CPD* cDNA probe. The DNA fingerprints show the presence of the *mas* promoter–cDNA junction (X) and *cpd*-specific fragments (B, C, and T), as well as the absence of the wild-type target site (A) in the complemented (cpd compl.) and *cpd* mutant lines. Other fragments detected by the cDNA probe correspond to six new T-DNA border fragments. Thus, the genetic segregation and DNA fingerprinting data indicate that, in the complemented line, tandem T-DNA copies of pPCV701 vector are present in three loci showing independent segregation. RNAs (right) were prepared from 14-day-old wild-type, *cpd* mutant, and complemented *cpd* plants and hybridized with the *CPD* cDNA probe.

(C) Comparison (top) of the phenotype of wild-type (left) and complemented *cpd* seedlings grown in soil under white light. Comparison (bottom) of the leaf morphology of wild type (first two leaves from the left) with that of *cpd* mutant (third leaf) and *CPD*-overexpressing complemented plants (three leaves at the right).

in the database with the conserved N-terminal membrane-anchoring, proline-rich, oxygen- and heme-binding domains of microsomal cytochrome P450s (Figure 5; 50%–90% sequence identity with conserved P450 domains defined by Nebert and Gonzalez, 1987). The *CPD* gene–encoded protein thus appeared to possess all functionally important domains of P450 monooxygenases (Pan et al., 1995). In addition, the sequence comparison also indicated a homology between CYP90 and specific domains of steroid hydroxylases. Members of the CYP2 family, including the rat testosterone-16α-hydroxylase (CYP2B1; 24% identity; Fujii-Kuriyama et al., 1982), showed sequence similarity with CYP90 in their central variable region (positions 135–249; Figure 5), carrying the steroid substrate-binding domains SRS2 and SRS3 (Gotoh, 1992). Moreover, in the CYP21 family, represented by the human progesterone-21-hydroxylase (CYP21A2; 19% identity; White et al., 1986), the positions of introns 7 and 8 corresponded to those of introns 3 and 5 in the *CPD* gene, suggesting a significant evolutionary relationship (Nelson et al., 1993). Nonetheless, because its overall sequence identity with other

P450s was less than 40%, the *CPD* gene product was assigned to a novel P450 family, CYP90, clustering on the evolutionary tree with CYP85 from tomato, CYP87 from sunflower (both unpublished data), and CYP88 from maize (Winkler and Helentjaris, 1995; P450 Nomenclature Committee, D. Nelson, personal communication).

Brassinolide and C23-Hydroxylated BR Precursors Restore the *cpd* Mutant Phenotype to Wild Type

These sequence homology data were, however, insufficient to predict the substrate specificity of CYP90 (Nelson et al., 1993). Therefore, the elongation response of the *cpd* mutant to all plant growth factors whose synthesis could involve P450 enzymes was tested. In these bioassays auxins, gibberellins, cytokinins, abscisic acid, ethylene, methyl-jasmonate, salicylic acid, and different retinoid acid derivatives (see Experimental Procedures) failed to promote the hypocotyl elongation of the *cpd* mutant grown in the dark or light (data not shown). However, brassinolide, an ecdysone-like plant steroid (used at concentrations of 0.005 to 1×10^{-6} M),

```
                    <              anchor reg.              >      < Pro dom.>
CYP90                              MAFTAELLLLLSSIAAGFLLLLRRTRYR----RMGLPPGSLG-LPLIGETEQL---IGA  50
CYP88    MLGVGMAAAVLLGAVALLLADAAARRAHWWYREAAEAVLYGAVALVVVDAAARRAHGWYREAALGAARRARLPPGEMG-WPLVGGWWAF--LRA  90
CYP71B1                    MDLLYIVAALVIFASLIIAKSKR--KPKKNLPPGPPRLLPIIGNLHOL---C-  47
CYP76A2              MEWEWSYVFFSALIILPAFILFFSQKNTTKSSYKEPPGPPG-LPIFGNMEEL---C-  52
CYP73                 MDLLLIEKTLVALFAAIIGAILISKTTGRHLPPGPRG-VPLFGNWLQV---C-  48
CYP2B1               MEPTILLLLALLVGFLLLLVRGHPKSRG---NEPPGPRP-LPLLGNLLQLDR-C-  49
CYP21A2              MLLLGLLLLLPLLAGARLLWNWWKLR----SLHLPPLAPCFLHLLQPDLPIYLLC-  51
                                                                    P        P  G          G
```

```
YKTENPEPFIDERVARYGSVEMTHLEGEPTIFSADPETNRFVLQNEGKLFECS------YPASICNLLGKHSLLLMKGSLHKRMHSLTMSFANSSIIKDHLMLDID  150
FKSGKPDAFIASFVRRFGRTGVYRSFMFSSPTVLVTTAEGCKQVLMDDDAFVT----GWPKATVALVGPRSFVAMPYDENRRIRKLTAAPINGFDALTGYLPFID  191
---EKPHRAMVELSKTYGPLMSLKLGSVTIVVATSVETVRDVLKTYDLEC-CSRPYMTYPARITYNLKDLV-FSPYDKYWRQVRKLTVVELYTAKRVQSFRHIRE  147
---TEPYKKMAVLRQKYGPVLWLKLGSTYIMVVQTAQASEELFKNHDISE-ANRVIPDVNQAHSYYQGSL-AIAPYGPFWRFQRRICTIEMFVHKKISETEPVRR  152
--DDLNHRNLTDLAKRFGEILLLRMGQRNLVVVSSPELAKEVLHTQGVEI-GSRTRNVVFDIFTGKGQDMV-FTVYGEHWRKMRRIMTVPFFTNKVVQQYRYGWE  150
-----LLNSFMQLREKYGDVFTVHLGPRPVVMLCGTDTIKEALVGQAEDE-SGRGTIAVIEPFKEYGVI-----------------FANGERWKALRRFSLA  128
-----------LTQKFGPIYRLHLGLQDVVVLNSKRTIEEAMVKKWADE-AGRPEPLTYKLVSRNYPDLSL-GDYSILWKAHKKLTRSALLLG-IRDSMEPVVE  140
                              G                               R              G
```

```
RL----VRFNLDS-WSSRV---LLMEEAKKITFELTVKQLMSFDPGE---------------------------------------WSESLRKEYLLVIEGFFSLPLPLF  213
RT----VTSSLRA-WADHG---GSVFLTELRRMTFKIIVQIFLGGA------------------------------------------DQATTRALERSYTELNYGMRAMAINLP  257
EEVASFVRFNKQA-ASSEE---TVNLSQKILKMSGSVICRIGFGINL--------------------------------------------EGSKLNTYQEIIVQAFE---VLGSLA  213
KCVDNMLKWIEKE-ANSAEKGSGIEVTRFVFLASFNMLGNLILSKDL------------------------------------------ADLESEEASEFFIAMKRINEWSGIAN  217
AEAAAVDDVKKNPAAATE---GIVIRRRLQLMYNNMFRIMFDRRF-----------------------------------------ESEDDPLFLKLKAL-NGERSRLA  216
TM----RDFGMGK-RSVEE---RIQEEAQCLVEELRKSQGAPPDETFLFQCITANIICSIVFGERFDYTDRQFLRLLELFYRTFSLLSSFSSQVFEFES-GLKYE  224
QL--TQEFCERMRAQPGTPV---AIEEEFSLLICSIICYLT--FGDKI--------------------------------------------KDDNLMPAYYKCIQEVLKTWSHWS  205
```

```
                                                                                dioxigen-bdg.
STTY--------------RKAIQARRKVAEALTVVVMKRREEEEGAERK---KDMLAALLAAD---------DGFSDEEIVDFLVALLVAGYETTSTIMTUAVK  292
GFAY--------------RGALRARRRLVAVLQGVLDERRAARAKGVSGG--GVDMMDRLIEAQ------DERGRHLDDDEIIDVMYLNAGFESSGHITMWATV  342
AVDYFPVIGTIIDRITGLHKCEK-------VFHGIDSFFDQAIQRHIDDPSIKDDIIDLLLKMERGEGSLGEYELTRPHTKGILMNILTAGIDTSAQTMIWAMT  310
VSDIFPFLKKFD-LQSLRKKMARDMG---KAVEIMSMFLKFRPEEERKKGTEKGKDFLDVLLEFQ-GTGKDEPAK-LSEHFIKIEVLEMFLAGIETTSSSVEWALT  323
QSFEYNYGDFIPILRPFLRNYLKLCKEVKDKRIQLFKDYFVDERKKIGST-KKMDNNQLKCAID-HILEAKEKGEINEDNVLYIVENINVAIETTLWSIEWGIA  320
PGAH--------------RQISKNLQEILDYIGHIVPKHRATLDPSAPRD----FIDTYLRME---KEKSNHHEEHHENLMISLLSLFFAGIETSSTTLRYGFL  308
IQIVDVIPFLRFFPNPGLRRLKQAIEKRDHIVEMQLRQHKESLVAGQWRD----MYDYMLQGVA-QPSMEEGSGQLLEGHVHMAAVDLLIGGTETTANTLSWAVV  306
                                                                         T
```

```
                            <        steroid bdg.        >
FLTSTPLALAQLKEEHDKIRAMK-SDSYSLEWSDYKSMPFTQCVVNETLRVANII-GGVFRRAMTDVEIKGYKIPKGWKVFSSFRAVHLDPNHFKDARTFNPWRW  395
FLQDNPDMFARAKAEQEAIMRSIPSSQRGLTLRDFRKMEYLSQVIDETLRLVNIS-FVSEROATRDVFVNGYLIPKGWKVQLWYRSVHMDPQVYEDPTKFDPSRW  446
HLLANPRVMKKLQAEIREKIKNI----DEITDDDVEQLDYFKLVLKETFRISPIVPVFLVPRVAAKDLKLPNGMKAEELSIEENYGLICVKKLPLEAIPVLTQWT  411
ELLRHPEAMAKVKTEISQAIEPN----RKFEDSDIENLPYMOAVLKESLRLHPPLPFLIPRETIQDTKFMGYDVPKDTQVLVNAWAIGRDPECWDDPMSEKPERF  424
ELVNHPEIQAKLRHELTDKLGPG----VQITEPDVQNLPYLQAVVKETLRLRMAHLPLLVPHMNLHDAKLGGFDIPAESKILVNAWWLANNPDQWKKPEEFRPERF  421
LMLKYPHVAEKVQKEIDQVIGSH-----RLPLDDRSKMPYTDAVIHEIQRFSDLVPIGVPHRVTKDTMFRGYLLPKNTEVY-PILSSALDPQYEDHPDSFNPEHF  407
FLLHHPEIQQRLQEELDHELGPG-ASSSRVPYKDHARLPLLNATIAEVLRLRPVVPLALPHRTTRPSSISGYDIPEGTVIIPNLQGAHLDETVWERPHEF----W  406
                          E                         KE R             P         GY  P      W         W       ERF
```

```
< heme-bdg. >
QNS---VTTGPSNVETPFGGGPRLCPGYELARVALSVFLHRLVTGFSW---VPAEQDKLVFFPTTRTQKRYPIFVKRRDFAT  472
EHS------PRAGTELAFGLGARLCPGNDLAKLEISVFLHHFLLGYKLARTNPRCRVRYLPHPRPVDNCLAKITRVGS  519
INQ--TDFKGLNFELLPFGGGPRMCPGMGLAVVHLTLINLLYRFDW--KLPNGMKAEELSIEENYGLICVKKLPLEAIPVLTQWT  496
LSK--IDVKGQHYGLIPFGAGRRMCVGLPLGHRMMHFALGSILREFEW--ELPDGVSPKSINMDGSMGVTARKRDSLKVIPKKA  505
LEEAKVEANSNDFRYLPFGVGRRSCPGIILALPILGITIGRLVQNSEL-LPPPGQSKIDTDEKGGQFSLHILKHSTIVAKPRSF  505
L--ANGALK-KSEAFMPESTGKRICLGEGIARNELFLFFTTILN-FSV--SSHLAPKDIDLTPKESGIGKIPPTYQICFSAR  484
PRF---LEPGKNSRALAFGCGARVCLGEPLARLELFVVLTRLLQAETL-LSSGDALPSLQPLPHCSVILKMQPFQVRLQPRGMGAHSPGQSQ  495
     FG  G  RC  G            L      F      P
```
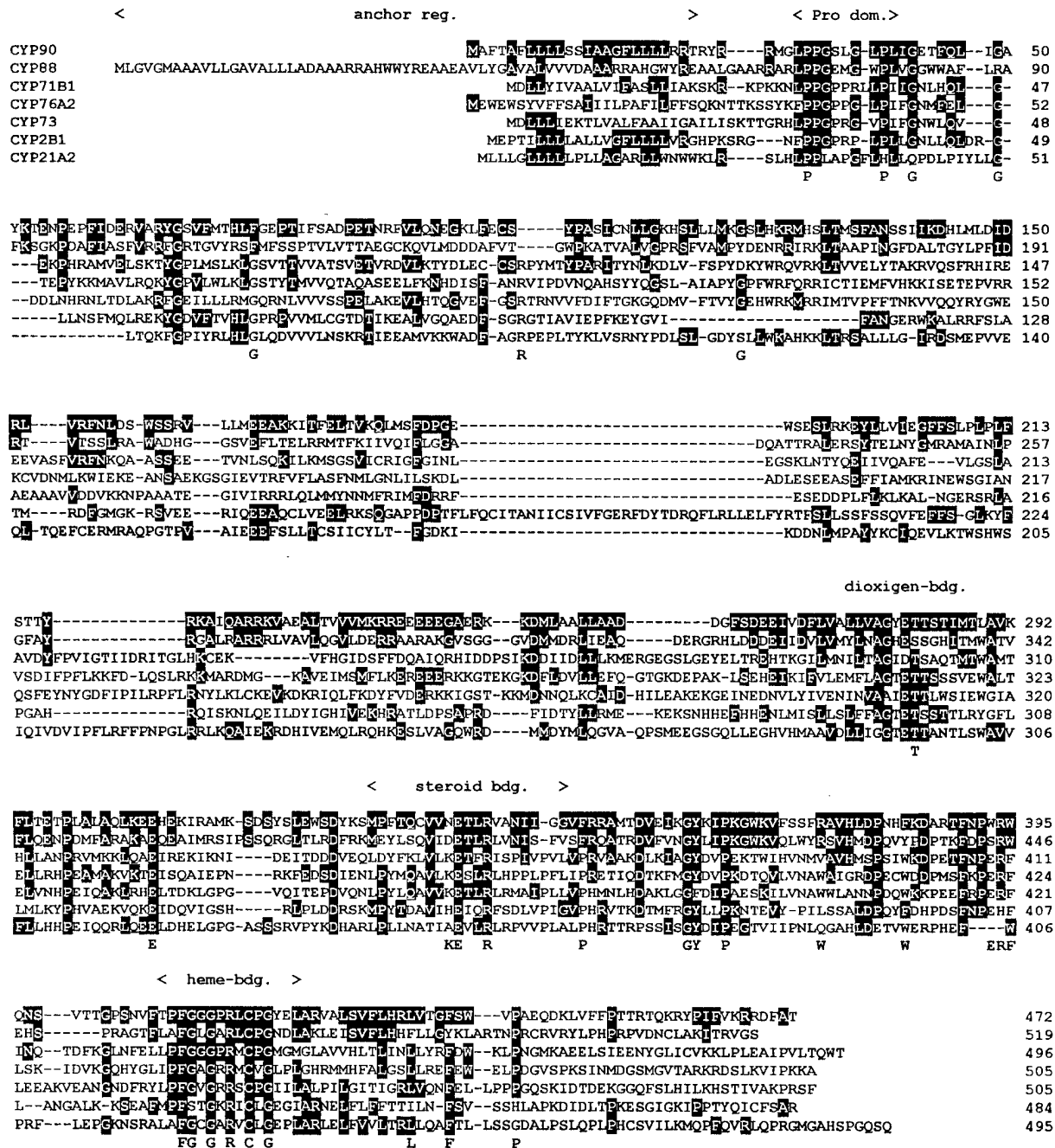
Figure 5. Sequence Homology between CYP90 and Other Cytochrome P450 Proteins from Plants and Animals

CYP90 shows the highest sequence identity (28%) with CYP88 (GA12→GA53 gibberellin 13-hydroxylase; Winkler and Helentjaris, 1995) from maize, but differs in several domains from other plant P450s, including CYP71B1 of Thlaspi arvense (23% identity; GenBank accession number L24438), CYP76A2 of eggplant (19% identity; GenBank X71657), and cinnamate 4-hydroxylase CYP73 of Jerusalem artichoke (17% identity; GenBank Z17369). CYP90 and CYP88 differ from all other plant P450s (Frey et al., 1995) by amino acid exchanges in the conserved positions G76, K337, P350, W375, W384, E393, and F396, as indicated below the sequence comparison. CYP90 also exhibits sequence homology to all conserved domains of animal P450s, such as CYP2B1 (GenBank J00719) and CYP21A2 (GenBank S29670) and also to the central variable region of CYP2 family (positions 135–249), which carries the substrate-binding domains SRS2 and SRS3 (Gotoh, 1992). The locations of conserved domains of microsomal P450s, including the membrane anchor region and the proline rich-domain, as well as the O_2-, steroid-, and heme-binding domains, are indicated by angle brackets above the aligned sequences. Identical amino acids are labeled by inverted printing.

was found to restore cell elongation in the hypocotyl, leaves, and petioles of *cpd* mutant seedlings in both dark and light. Brassinolide treatment also restored the male fertility of the mutant, allowing the production of homozygous seeds.

When grown in the presence of C23-hydroxylated BR
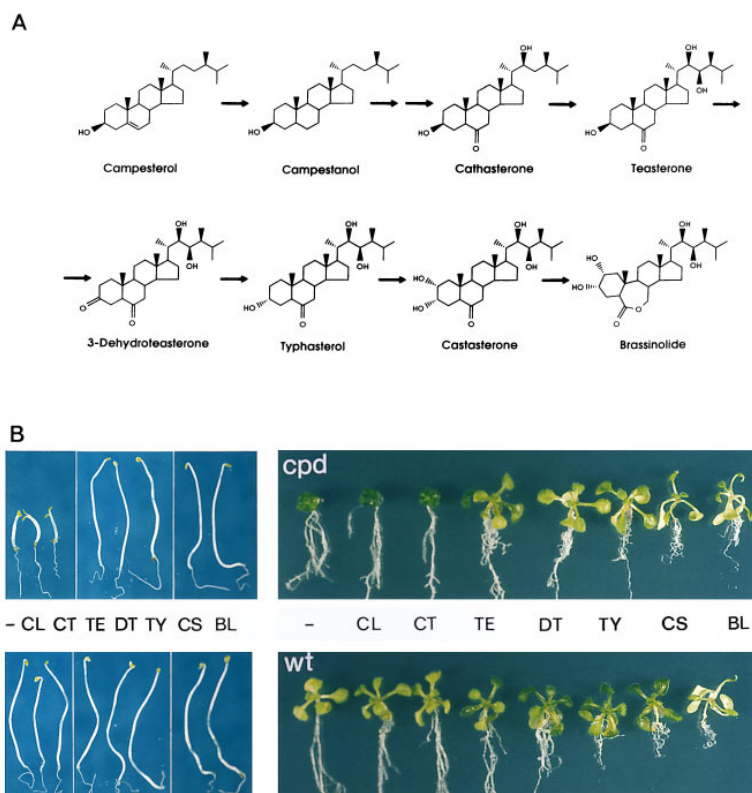
A

B

Figure 6. BRs Restore the *cpd* Mutant Phenotype to Wild Type

(A) Biosynthesis pathway of BRs (Fujioka et al., 1995).

(B) Wild-type (wt) and *cpd* mutant seedlings were grown for 5 days in the dark (left) or for 14 days in the light (right) with no steroid (minus) or with 0.2×10^{-6} M of campesterol (CL), cathasterone (CT), teasterone (TE), 3-dehydroteasterone (DT), typhasterol (TY), castasterone (CS), or brassinolide (BL).

precursors (0.1×10^{-6} to 1×10^{-6} M) of brassinolide, such as teasterone, 3-dehydroteasterone, typhasterol, and castasterone (Fujioka et al., 1995), the *cpd* mutant was also indistinguishable from wild type in both dark and light (Figure 6). However, cathasterone and its precursor campesterol (as well as campestanol, 6α-hydroxycampestanol, 6-oxocampestanol, Δ²²-6-oxocampestanol, and 22α,23α-epoxy-6-oxocampestanol; data not shown), which do not carry a hydroxyl moiety at the C23 position, did not alter the *cpd* phenotype, suggesting a deficiency of cathasterone C23 hydroxylation to teasterone in the *cpd* mutant. From the synthetic [22*R*,23*R*,24*R*] derivatives of BRs (Adam and Marquardt, 1986), epi-teasterone was found to be inactive, whereas epi-castasterone and epi-brassinolide rescued the *cpd* phenotype as well as their [22*R*,23*R*,24*S*] stereoisomers.

Remarkably, the hypocotyl elongation response of wild-type seedlings was unaffected by BRs in the dark (Figure 6), indicating a possible saturation of this growth response. In contrast, treatments of wild-type seedlings with castasterone and brassinolide in the light promoted hypocotyl elongation (albeit with different efficiencies). When applied at higher concentrations (0.1×10^{-6} to 1×10^{-6} M), castasterone and brassinolide (as well as their epi-stereoisomers, but not other BRs precursors) caused aberrant leaf expansion, epinasty, senescence, and retarded development in both wild-type and mutant plants grown in the light (Figure 6).

The Effect of BRs on Other Arabidopsis Hypocotyl Elongation Mutants

The effect of castasterone and brassinolide (and their epi-isomers) on different Arabidopsis mutants impaired

in hypocotyl elongation was similarly tested. To avoid complexity resulting from negative regulation of the hypocotyl elongation by light, the mutants were germinated in the presence or absence of BRs in the dark, and their hypocotyl growth was compared with that of untreated and ergosterol-treated seedlings as controls (Figure 7). Mutants in gibberellin biosynthesis (*ga5*) or perception (*gai*), showing dwarfism and inhibition of hypocotyl or epicotyl growth (or both) in the light (Finkelstein and Zeevaart, 1994), developed hypocotyls similar to or shorter than the wild type, but did not respond to BRs by significant (>20%) hypocotyl elongation in the dark. The inhibition of hypocotyl growth in the dark-grown ethylene-overproducing mutant *eto1* (Ecker, 1995) was also unaffected by BRs. In contrast, BR treatments stimulated the rate of hypocotyl elongation by 50%–80% in the ethylene-resistant mutant *etr1* (Ecker, 1995). The hypocotyl elongation of the auxin/ethylene-resistant *axr2* mutant (Estelle and Klee, 1994) was also increased 2- to 3-fold by BRs, which promoted the enlargement of cotyledons but inhibited the root growth of *axr2* seedlings. The wild type and the *ga5*, *gai1*, *eto1*, *etr1*, and *axr2* mutants displayed comparable hypocotyl elongation, but different epicotyl/stem growth, responses to BRs in the light.

As was observed for the *cpd* mutant, castasterone and brassinolide restored the phenotype of the *dim* mutant (Takahashi et al., 1995) to wild type in the dark, as well as in the light (data not shown). In contrast, the hypocotyl elongation of *det1*, *cop1-16*, *fus4*, *fus5*, *fus6*, *fus7*, *fus8*, *fus9*, *fus11*, and *fus12* mutants (Chory and Susek, 1994; Deng, 1994; Miséra et al., 1994) was stimulated 3- to 10-fold by BRs only in the dark. BRs inhibited
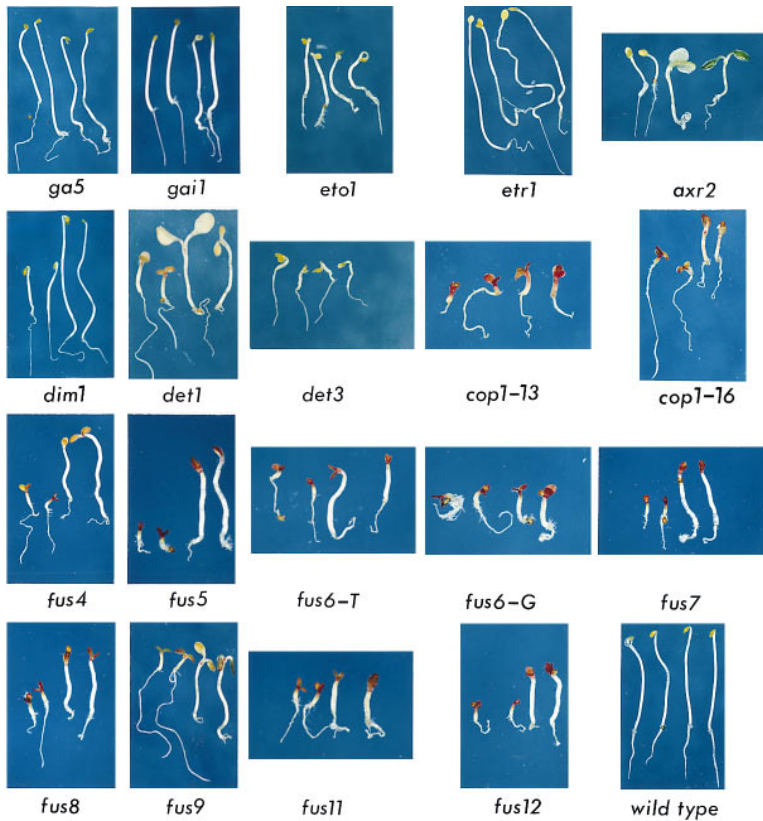
Figure 7. The Effect of BRs on the Hypocotyl Elongation of Dark-Grown Arabidopsis Mutants

Each picture shows seedlings grown for 5 days in the dark. From left to right, the first seedling was grown in the absence of steroid, the second was treated with ergosterol, the third with epi-castasterone, and the fourth with epi-brassinolide. The concentration of steroids was 0.1×10^{-6} M. (Before the pictures were taken, the seedlings were inspected under the microscope, which explains the greening of cotyledons in certain mutants.)

the elongation of roots in these mutants. BRs also stimulated the cell enlargement and decreased the accumulation of anthocyanins in the cotyledons of *det1* and *fus9* mutants. In comparison with their alleles, the *cop1-13* and *fus6-G* mutants showed no hypocotyl elongation response or a minimal response (10%–20%) to castasterone and brassinolide, respectively, whereas the *det3* mutant (Chory and Susek, 1994) was found to be completely insensitive to BRs.

Discussion

BRs Are Required for Plant Cell Elongation
Since their discovery (Grove et al., 1979), BRs have been considered to be nonessential plant hormones because their concentration is extremely low in most plant species and their action spectrum is redundant with those of the ubiquitous growth factors auxin, gibberellin, ethylene, and cytokinin. A major argument supporting this view is that BRs are inactive in hypocotyl elongation assays performed in the dark, which are used as standard tests to monitor the activity of photoreceptors and phytohormones controlling cell elongation (for review see Davies, 1987; Kendrick and Kronenberg, 1994). The data described above clearly undermine this argument, since they demonstrate that the phenotype of a hypocotyl elongation mutant can be restored to wild type by brassinolide and its precursors, but not by other known plant growth factors. The BR precursor feeding experiments suggest that the hypocotyl elongation defect in the *cpd* mutant results from a deficiency in brassinolide biosynthesis.

Brassinolide has been observed in many plant species to stimulate the longitudinal arrangement of cortical microtubuli and cellulose microfilaments, leaf unrolling, xylem differentiation, and hypocotyl elongation in the light. Brassinolide is also reported to inhibit root elongation, radial growth of the stem, anthocyanin synthesis, and de-etiolation (Mandava, 1988). Phenotypic traits of the *cpd* mutant, such as the inhibition of longitudinal cell elongation in most organs, the transverse arrangement of cellulose microfilaments on the surface of epidermal cells, the inhibition of leaf unrolling and xylem differentiation, and the induction of de-etiolation in the dark, are consistent with a phenotype expected for a mutant in brassinolide synthesis. In addition, the conservation of exon–intron boundaries between the *CPD* gene and CYP21 gene family of progesterone side chain hydroxylases, the homology of the CYP90 protein with all conserved domains of functional P450 monooxygenases, and the similarity of CYP90 domains with the substrate-binding regions of CYP2 testosterone hydroxylases also suggest that the *CPD* gene may code for a cytochrome P450 steroid hydroxylase.

Cytochrome P450s are known to use a wide range of artificial substrates in vitro, but perform well-defined stereo-specific reactions in vivo. Because their substrate specificity can be altered by mutations affecting the substrate-binding domains, the specificity of P450 enzymes can only be determined by in vivo feeding experiments with labeled substrates (Nebert and Gonzalez, 1987). Because it usually cannot be excluded that multiple cytochrome P450s contribute to a given metabolic conversion in vivo, such an analysis requires either

the overexpression of cytochrome P450s in transgenic organisms or mutants deficient in particular P450s. The *cpd* mutant and *CPD*-overexpressing transgenic plants therefore provide suitable material to confirm the requirement of CYP90 for C23 hydroxylation of cathasterone in brassinolide biosynthesis (Fujioka et al., 1995).

Hypocotyl Elongation Mutants Affected in BR Responses

Physiological data indicate that the biosynthesis of gibberellins and steroids involves common precursors (Davies, 1987) and that BRs stimulate ethylene biosynthesis in the light (Mandava, 1988). Nonetheless, mutants affected in ethylene production (*eto1*), gibberellin biosynthesis (*ga*), and perception (*gai*) do not respond to BRs in the dark, and BRs promote only a weak hypocotyl elongation response in the ethylene-resistant *etr1* mutant. Thus, mutants affected in ethylene, gibberellin, and BR responses can clearly be distinguished. The BR bioassays performed with *cpd* mutant and wild-type Arabidopsis seedlings in the dark show that BR deficiency can result in a short hypocotyl phenotype, although BRs do not stimulate hypocotyl elongation in the wild type. Mutants deficient in BR biosynthesis are expected, therefore, to develop short hypocotyls, which should be restored to wild type by brassinolide and BR precursors. One can also predict that mutants defective in BR perception or signaling (or both) will show short hypocotyl and a partial or complete insensitivity to BRs.

The phenotype of the *dim* mutant, like that of *cpd*, is restored to wild type by castasterone and brassinolide in both dark and light, suggesting that *dim* may also be impaired in BR biosynthesis. The de-etiolated mutant *det2* also appears to be a BR biosynthetic mutant. The *DET2* gene codes for a homolog of animal steroid-5α-reductases that is probably required for the conversion of campesterol to campestanol in the first step of brassinolide biosynthesis (J. Li, P. Nagpal, V. Vitart, and J. Chory, personal communication). In other de-etiolated and constitutive photomorphogenic mutants, such as *det1*, *cop1-16*, *fus4*, *fus5*, *fus6*, *fus7*, *fus8*, *fus9*, *fus11*, and *fus12*, BRs stimulate hypocotyl elongation only in the dark. The *cop1-13* mutant, which produces no COP1 protein (McNellis et al., 1994), is apparently insensitive to BRs. In contrast, the less severe *cop1-16* mutant (McNellis et al., 1994; Miséra et al., 1994), synthesizing an immunologically detectable amount of mutant COP1 protein, responds to BRs by hypocotyl growth. The *fus6* mutant displays similar allelic differences, whereas the *det3* mutant shows a complete insensitivity to BRs. It is therefore possible that these mutations affect regulatory functions involved in BR perception, signaling, or both.

The Effect of the *cpd* Mutation and *CPD* Overexpression on Gene Expression

The *cpd* and *det2* mutations result in similar phenotypic traits, including the induction of de-etiolation and expression of light-induced *RBCS* and *CAB* genes in the dark. Thus, *cpd* can be considered to be a novel type of *det* mutation. Genetic analyses of *det/hy* double mutants suggest that *det1* and *det2* are epistatic to the *hy* mutations of photoreceptors. Therefore, *det1* and *det2* have

been proposed to act in parallel light-signaling pathways as negative regulators of de-etiolation (Figure 8) (Chory and Susek, 1994). In the *det1* pathway, the products of *DET1*, *COP1*, and some *FUS* genes are thought to function as nuclear repressors of light-regulated genes in the dark (Deng, 1994; Quail et al., 1995). Now, the putative *det2* light-signaling pathway (Chory and Susek, 1994) appears to be a BR pathway, because *det2* as well as *cpd* and *dim* mutants are restored to wild type by BRs. This is consistent with data indicating that BRs inhibit de-etiolation in the dark (Mandava, 1988). Our data also show that the *cpd* mutation results in the activation of stress-regulated *CHS*, alcohol dehydrogenase, *HSP18.2*, lipoxygenase, and S-adenosylmethionine synthase genes in the light. This correlates with the observations showing that BRs suppress anthocyanin synthesis (i.e., controlled by *CHS*; Mandava, 1988) and that the *CHS* gene is also induced in the *det2* mutant (Chory et al., 1991). The *CPD* function (and thus the *det2*/BR pathway) appears therefore to regulate stress signaling negatively, possibly via the modulation of lipoxygenase involved in the generation of lipid hydroperoxide signals (e.g., jasmonate), which are known to control defense and stress responses in plants (Farmer, 1994). Cytokinin treatment of wild-type Arabidopsis has been observed to result in a phenocopy of the *det2* mutation (Chory et al., 1994). In agreement, our data show that the transcription of the *CPD* gene is downregulated by cytokinin, which may thus control BR biosynthesis. The expression of the *CPD* gene is also modulated by light and the availability of carbon source (e.g., sucrose), suggesting complex regulatory interactions between light and BR signaling. It is therefore possible that the *cpd* and *det2* mutations only indirectly affect the expression of light-regulated genes (e.g., through the regulation of stress responses). Studies of the *dim* mutant indicate that inhibition of the hypocotyl elongation may not influence the expression of light-induced *RBCS*, *CAB*, and *CHS* genes in the dark (Takahashi et al., 1995). This is intriguing, because the phenotypic traits of the *dim* mutant are nearly identical with those of the *cpd* and *det2* mutants, and our precursor feeding experiments suggest that *dim* causes a deficiency before typhasterol in BR biosynthesis (our unpublished data). A comparative analysis of *det2*, *cpd*, and *dim* mutants, including their combinations with *hy* loci, is therefore necessary to clarify how the regulation of light-induced genes is affected by brassinolide or its BR precursors (or both).

Unlike *det2*, the *dim* mutation has been proposed to control cell elongation by specific regulation of the tubulin *TUB1* gene expression (Takahashi et al., 1995). In fact, the available genetic data do not prove that the signaling pathways identified by the *det1* and *det2* mutations are exclusively involved in light signaling (Millar et al., 1994). Therefore, *DET*, *COP*, *FUS*, and *CPD* genes can also be considered to act as positive regulators of cell elongation, because their inactivation results in the inhibition of hypocotyl elongation. The fact that BRs can compensate for the cell elongation defects caused by the *det1*, *cop1*, and *fus*, as well as *det2*, *cpd*, and *dim*, mutations suggests some interaction between the *det1* and *det2* pathways. BR insensitivity of the *cop1-13* null
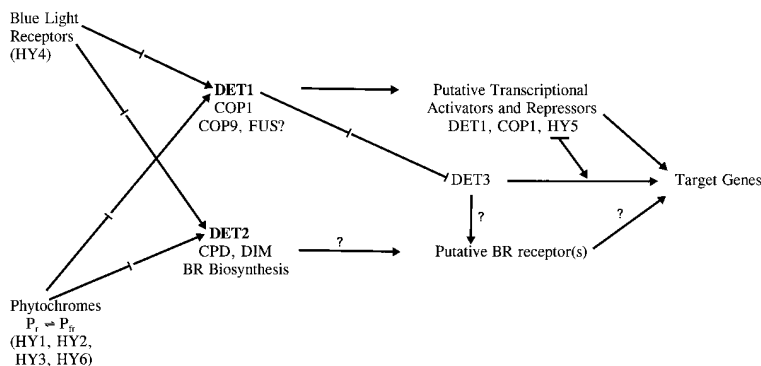
Figure 8. A Genetic Model for Independently Acting *det1* and *det2* Signaling Pathways

This model, advanced by Chory and Susek, proposes the following: first, *DET1*, *COP1*, and *COP9* are negative regulators of de-etiolation; second, light signals activating phytochromes (P_r to P_{fr}) and/or blue light receptors (such as HY4) decrease the activity of *DET1* (*COP1* or *COP9*), causing derepression of light-regulated developmental and gene expression responses; third, the *HY5* function acts downstream of *DET1*; fourth, *det3* is epistatic to *det1*; and fifth, *DET2* is a negative regulator of de-etiolation (photomorphogenesis) acting downstream of phytochromes and

blue light receptors. The *det2* pathway is thought to be independent of *det1*, because the phenotypes of *det2hy5*, *det1det2*, and *det2det3* double mutants appeared to be additive. Negative regulatory interactions proposed by this model are marked in the scheme by interrupted arrows. Data of the epistasis analysis resulting in this model were critically discussed by Millar et al. (1994). The *det1*, *det2*, and *det3* mutants all display short hypocotyl in the dark; thus, scoring the phenotypes of double mutants is rather difficult. Millar et al. (1994) noted that if a mutation affects the biosynthesis of a signaling molecule, the epistasis data are not sufficient to establish the order of functions combined. In fact, *det2* (as well as *cpd* and *dim*) now define the biosynthetic pathway of BR hormones. Therefore, the phenotypes of *det* double mutants may not be informative, because *det3* is insensitive to BRs, whereas the short hypocotyl phenotype of the *det1* mutant is altered by BRs in the dark. (If *det1*, *det2*, or *det3* were null mutations, the phenotype of one of the combined mutations should not be altered in the double mutants.) A role for putative steroid receptors, as well as for possible transcriptional repressors (DET1 and COP1) and activators (HY5), has been added to the original model of Chory and Susek (1994).

mutant may indeed point to a possible involvement of the COP1 WD protein (Deng et al., 1992) in BR responses. These observations clearly suggest that further studies are needed to confirm the proposed model of independently acting *det1* and *det2* pathways (Figure 8) (Chory and Susek, 1994), including the identification of an as yet unknown plant steroid receptor(s) and the functional characterization of *DET*, *COP*, and *FUS* gene products. Nonetheless, this genetic model can already be extended by considering possible regulatory interactions between the *DET*, *COP*, *FUS*, *DIM*, and *CPD* genes and their products, as well as their effects on signaling by light, stress, and steroids and in response to pathogen attack.

Pleiotropic effects of the *cpd* mutation also suggest a possible involvement of CYP90 protein in multiple signaling pathways. Remarkably, overexpression of *CPD* mRNA in the genetically complemented lines results in the activation of pathogenesis-related *PR* genes (Uknes et al., 1992), which are inducible in Arabidopsis by superoxide radical and H_2O_2 signals (Mehdy, 1994). The induction of *PR* genes, however, may not necessarily reflect an overproduction of BRs. In plants, the membrane-associated cytochrome P450s occur in complexes with cytochrome b5 and NAD(P)H-oxidoreductases (Crane et al., 1993), which, in the absence of substrate saturation, can transfer electrons to O_2, yielding superoxide radicals. Thus, the induction of *PR* genes may also result from the overexpression of CYP90 protein itself. In any case, further genetic studies of the *cpd* mutant and functional analysis of the CYP90 protein should answer these open questions and provide further insight into basic functions of BRs in the regulation of plant development.

Experimental Procedures

Genetic Analysis

The *cpd* mutant was identified by screening for hypocotyl elongation defects in a T-DNA insertional mutant collection generated by tissue

culture transformation of Arabidopsis with Agrobacterium Ti plasmid derived vectors as described (Koncz et al., 1989, 1992b). Properties and application of the T-DNA vector pPCV5013Hyg were reported earlier (Koncz et al., 1989, 1994). For trisomic analysis and linkage mapping, a *cpd*/+ line was crossed with the tester lines as described (Koncz et al., 1992b) and hygromycin resistant F1 hybrids were selected by germinating seeds in MS medium for Arabidopsis (MSAR medium) (Koncz et al., 1994).

After outcrossing of the *cpd* mutant with wild type, eight F2 families yielded an offspring of 1297 wild-type and 437 dwarf plants (2.97:1), fitting (χ^2 0.037; homogeneity: 2599; P = 0.85) the expected 3:1 ratio for monogenic segregation of the recessive *cpd* mutation. From these F2 families, 5383 mutants were tested on hygromycin and all displayed resistance, indicating a tight linkage between the T-DNA insertion and the *cpd* mutation.

In contrast to other trisomic hybrids, segregating the mutation at a ratio of 3:1, the chromosome 5 trisomic tester T31 produced an aberrant F2 ratio of 588 wild-type (336 resistant and 252 sensitive to hygromycin) and 60 *cpd* mutant (all hygromycin resistant) plants. The ratios of wild type to mutant (9.8:1) and hygromycin resistant to sensitive (1.57:1) progeny matched with the ratios expected for synteny (8:1 and between 1.25:1 and 2.41:1, respectively).

The T-DNA insert and the *cpd* mutation were simultaneously mapped, using the *ttg* marker of chromosome 5 in repulsion. For determination of the *cpd–ttg* map distance, two mapping populations were raised, one including plants grown in soil and another using seedlings germinated in MSAR medium and tested in the presence of 15 μg/ml hygromycin. The soil-grown population was scored for the hairless *ttg* and dwarf *cpd* phenotypes in F2, and seeds from fertile plants were carried to full F3 analysis. By labeling *cpd* as "a" and *ttg* as "b," the actual scores in the soil-grown population were 1054 AaBb, 685 aaB. (424 aaBB and 261 aaBb by extrapolation), 387 AAbb, 261 aAbb, 248 AaBB, 251 AABb, 21 AABB, and 25 aabb. Progeny analysis showed that the AaBb, aAbb, AaBB, and aabb classes were hygromycin resistant, in contrast to the hygromycin-sensitive classes AAbb, AABb, and AABB. In the population scored on MSAR medium with controlled seed germination, the data were 815 AaB., 512 aaB., 193 AAB, 300 AAbb, 159 aAbb, and 17 aabb. Both mapping populations yielded identical frequencies for the double recombinant fraction (*cpd–ttg*). The recombination frequencies and derived map distances were calculated by the maximum likelihood method as described (Koncz et al., 1992a). From these data the smaller map distance, corrected for the error resulting from uneven seed germination in soil, was accepted, resulting in 21.18 $\pm$ 0.86 cM (centimorgans) for the *cpd*(5-14.3)–*ttg*(5-35.5) interval. By scoring 1520 recombinant chromosomes, no crossing-over

between the T-DNA-encoded hygromycin resistance marker and the *cpd* mutation was found, indicating that the T-DNA insertion was located in the *cpd* locus.

Physical Mapping and Characterization of the *CPD* Gene and Its Effects on Gene Expression

To isolate the T-DNA-tagged locus, a genomic DNA library was constructed by ligation of *cpd* DNA, digested partially by MboI, into the BamHI site of the λEMBL 3 vector (Sambrook et al., 1989). Following the physical mapping of the λEMBL3 clones, the T-DNA–plant DNA juntion fragments (flanked by BamHI and HindIII sites in the plant DNA, see Figure 3A) were used as probes for the isolation of 4 genomic and 4 cDNA clones from wild-type Arabidopsis λEMBL4 genomic and λgt10 cDNA libraries. These clones were mapped and their fragments were subcloned and sequenced, in order to characterize the *CPD* cDNA (EMBL X87367) and gene (EMBL X87368). The 5′ end of the *CPD* transcript of 1735 bases was mapped 166 bp upstream of the ATG codon (data not shown), whereas the polyadenylation signal was located 104 nucleotides downstream of the stop codon in the 3′ UTR of 131 bases.

For genetic complementation of the *cpd* mutation, the longest *CPD* cDNA (extending 47 bp ustream of the ATG codon) was cloned into the BamHI-site of plant expression vector pPCV701, conjugated from E. coli to Agrobacterium, and transformed into the homozygous *cpd* mutant by Agrobacterium-mediated Arabidopsis transformation as described (Koncz et al., 1994). To identify yeast artificial chromosome clones containing the *CPD* locus, wild-type Arabidopsis YAC libraries were screened by hybridization (Koncz et al., 1992b), using the *ocs* T-DNA–plant DNA junction fragment (BamHI–EcoRI fragment in Figure 3A) as a probe.

DNA analyses and cloning, screening of lambda phage libraries, DNA and RNA filter hybridizations and sequencing of double-stranded DNA templates were performed using standard molecular techniques (Sambrook et al., 1989). For hybridization of RNA blots, the following cDNA probes were used: *RBCS* (EST ATTS0402, GenBank [gb]: X13611), *CAB140* (Ohio Arabidopsis Stock Center (OASC) 38A1T7, gb A29280), alkaline peroxidase (EST ATTS0366, gb P24102), nonchloroplastic *SOD* (OASC 2G11T7P), *GST2* (gb L11601), *HSP70* (gb M23108), lignin-forming peroxidase (EST ATTS0592, gb P11965), *CHS* (Trezzini et al. 1993), lipoxygenase (*Lox2*, gb L23968), S-adenosylmethionine synthase (OASC 40G2T7, gb P23686), *HSP18.2* (gb X17295), *ADH* (gb M12196), *PR1*, *PR2*, and *PR5* (Uknes et al., 1992). The RNA blot shown in Figure 3B was hybridized with plant DNA sequences flanking the *hpt*-pBR segment of the T-DNA (PstI–HindIII fragment in Figure 3A). The analysis of *CPD* DNAs and derived protein sequences was performed using the GCG and BLAST computer programs (Deveraux et al., 1984; Altschul et al., 1990), as well as P450 sequence compilations (Gotoh, 1992; Nelson et al., 1993; Frey et al., 1995).

Complementation of Arabidopsis Mutants with BRs and Other Plant Growth Factors

Plant growth factors including auxins (indole-3-acetic acid, α-naphthaleneacetic acid, 2,4-dichloro-phenoxyacetic acid), cytokinins (6-benzyl-aminopurine, 6-furfurylaminopurine, 6-(γ,γ-dimethylallylamino)-purine riboside), abscisic acid, salicylic acid, methyl-jasmonate, as well as retinoic acid derivatives (vitamin A aldehyde, 9-*cis*-retinal, 13-*cis*-retinal, trans-retionoic acid, 13-*cis*-retinoic acid, and retinol) were used at final concentrations of 0.01, 0.05, 0.1, 0.5, or 1 μM, whereas gibberellins (gibberellic acid GA3, GA4, GA7, and GA13) were applied at 0.1, 1, 10, and 100 μM concentrations in MSAR seed germination media.

BRs listed in Figure 6 and epi-isomers of teasterone, typhasterol, castasterone, and brassinolide were obtained from A. Sakurai and S. Fujioka (Institute of Physical and Chemical Research [RIKEN], Japan) and G. Adam (Institute for Plant Biochemistry, Halle, Germany). BRs were tested at similar concentrations (0.005, 0.01, 0.05, 0.1, 0.5, and 1 μM) in MSAR media used for seed germination under aseptic conditions (Koncz et al., 1994). The bioassays were evaluated after 1, 2, 5, and 10 days of germination by measurement of the length of hypocotyls and roots, as well as by visual inspection and photography of seedlings. Mutant plants grown in soil were sprayed with 0.1 or 1 μM aqueous solutions of castasterone or brassinolide.

Histological analyses were performed according to standard procedures (Feder and O'Brien, 1968). Tissues were fixed in formalin:acetic acid:ethanol (90:5:5), embedded in 2-hydroxyethyl methacrylate, sectioned at 10 μm using a rotary microtome, and stained by toluidine blue. To prepare contact imprints, seedlings were placed in 3% molten agarose and carefully removed from the solidified carrier before taking pictures. Arabidopsis mutants used in our studies were obtained from the Ohio and Nottingham Arabidopsis Stock Centers, as well as being donated by S. Miséra (Institute for Plant Genetics, Gatersleben, Germany).

References

Adam, G., and Marquardt, V. (1986). Brassinosteroids. Phytochem. *25*, 1787–1799.

Altschul, S.F., Gish, W., Miller, W., Myers, E.W., and Lipman, D.J. (1990). Basic local alignment search tool. J. Mol. Biol. *215*, 403–410.

Castle, L.A., and Meinke, D.W. (1994). A *FUSCA* gene of *Arabidopsis* encodes a novel protein essential for plant development. Plant Cell *6*, 25–41.

Chory, J., and Susek, R.E. (1994). Light signal transduction and the control of seedling development. In Arabidopsis, E.M. Meyerowitz, and C.R. Somerville, eds. (Cold Spring Harbor, New York: Cold Spring Harbor Laboratory Press), pp. 579–614.

Chory, J., Nagpal, P., and Peto, C. (1991). Phenotypic and genetic analysis of *det2*, a new mutant that affects light-regulated seedling development in *Arabidopsis*. Plant Cell *3*, 445–459.

Chory, J., Reinecke, D., Sim, S., Washburn, T., and Brenner, M. (1994). A role for cytokinins in de-etiolation in *Arabidopsis*. Plant Physiol. *104*, 339–347.

Crane, F.L., Morré, D.J., and Löw, H.E. (1993). Oxidoreduction at the Plasma Membrane: Relation to Growth and Transport, Volume 2 (Boca Raton, Florida: CRC Press).

Davies, P.J. (1987). Plant Hormones and Their Role in Plant Growth and Development (Dordrecht, The Netherlands: Martinus Nijhoff).

Deng, X.-W. (1994). Fresh view of light signal transduction in plants. Cell *76*, 423–426.

Deng, X.-W., Matsui, M., Wei, N., Wagner, D., Chu, A.M., Feldmann, K.A., and Quail, P.H. (1992). *COP1*, an Arabidopsis regulatory gene, encodes a protein with both a zinc-binding motif and a G_β homologous domain. Cell *71*, 791–801.

Deveraux, J., Haeberli, P., and Smithies, O. (1984). A comprehensive set of sequence analysis programs for the VAX. Nucleic Acids Res. *12*, 387–395.

Ecker, J.R. (1995). Ethylene signal transduction pathway in plants. Science *268*, 667–675.

Estelle, M., and Klee, H.J. (1994). Auxin and cytokinin in *Arabidopsis*. In Arabidopsis, E.M. Meyerowitz and C.R. Somerville, eds. (Cold

Spring Harbor, New York: Cold Spring Harbor Laboratory Press), pp. 555–578.

Farmer, E.E. (1994). Fatty acid signalling in plants and their associated microorganisms. Plant Mol Biol. 26, 1423–1437.

Feder, N., and O'Brien, T.P. (1968). Plant microtechnique: some principles and new methods. Am. J. Bot. 55, 123–142.

Finkelstein, R.R., and Zeevaart, J.A.D. (1994). Gibberellin and abscisic acid biosynthesis and response. In Arabidopsis, E.M. Meyerowitz and C.R. Somerville, eds. (Cold Spring Harbor, New York: Cold Spring Harbor Laboratory Press), pp. 523–553.

Frey, M., Kliem, R., Saedler, H., and Gierl, A. (1995). Expression of a cytochrome P450 gene family in maize. Mol. Gen. Genet. 246, 100–109.

Fujii-Kuriyama, Y., Mizukami, Y., Kawajiri, K., Sogawa, K., and Muramatsu, M. (1982). Primary structure of a cytochrome P-450: coding nucleotide sequence of phenobarbital-inducible cytochrome P-450 cDNA from rat liver. Proc. Natl. Acad. Sci. USA 79, 2793–2797.

Fujioka, S., Inoue, T., Takatsuto, S., Yanagisawa, T., Yokota, T., and Sakurai, A. (1995). Identification of a new brassinosteroid, cathasterone, in cultured cells of Catharanthus roseus as a biosynthetic precursor of teasterone. Biosci. Biotech. Biochem. 59, 1543–1547.

Gotoh, O. (1992). Substrate recognition sites in cytochrome P450 family 2 (CYP2) proteins inferred from comparative analyses of amino acid and coding nucleotide sequences. J. Biol. Chem. 267, 83–90.

Grove, M.D., Spencer, G.F., Rohwedder, W.K., Mandava, N.B., Worley, J.F., Warthen, J.D., Steffens, G.L., Flippen-Anderson, J.L., and Cook, J.C. (1979). A unique plant growth promoting steroid from Brassica napus pollen. Nature 281, 216–217.

Hauge, B.M., Hanley, S.M., Catinhour, S., Cherry, J.M., Goodman, H.W., Koornneef, M., Stam, P., Chang, C., Kempin, S., Medrano, L., and Meyerowitz, E.M. (1993). An integrated genetic/RFLP map of the Arabidopsis thaliana genome. Plant J. 3, 745–754.

Kendrick, R.E., and Kronenberg, G.H.M. (1994). Photomorphogenesis in Plants (Dordrecht, The Netherlands: Kluwer Academic).

Koncz, C., Martini, N., Mayerhofer, R., Koncz-Kalman, Z., Körber, H., Rédei, G.P., and Schell, J. (1989). High-frequency T-DNA-mediated gene tagging in plants. Proc. Natl. Acad. Sci. USA 86, 8467–8471.

Koncz, C., Chua, N.-H., and Schell, J. (1992a). Methods in Arabidopsis Research. (Singapore: World Scientific).

Koncz, C., Németh, K., Rédei, G.P., and Schell, J. (1992b). T-DNA insertional mutagenesis in Arabidopsis. Plant Mol. Biol. 20, 963–976.

Koncz, C., Martini, N., Szabados, L., Hrouda, M., Bachmair, A., and Schell, J. (1994). Specialized vectors for gene tagging and expression studies. In Plant Molecular Biology Manual, S.B. Gelvin and R.A. Schilperoort, eds. (Dordrecht, The Netherlands: Kluwer Academic), B2, pp. 1–22.

Mandava, B.N. (1988). Plant growth-promoting brassinosteroids. Annu. Rev. Plant Physiol. Plant Mol. Biol. 39, 23–52.

McNellis, T.W., von Armin, A.G., Araki, T., Komeda, Y., Miséra, S., and Deng, X.-W. (1994). Genetic and molecular analysis of an allelic series of cop1 mutants suggests functional roles for multiple protein domains. Plant Cell 6, 487–500.

Mehdy, M.C. (1994). Active oxygen species in plant defense against pathogens. Plant Physiol. 105, 467–472.

Millar, A.J., McGrath, R.B., and Chua, N.-H. (1994). Phytochrome phototransduction pathways. Annu. Rev. Genet. 28, 325–349.

Miséra, S., Müller, A.J., Weiland-Heidecker, U., and Jürgens, G. (1994). The FUSCA genes of Arabidopsis: negative regulators of light responses. Mol. Gen. Genet. 244, 242–252.

Nebert, D.W., and Gonzalez, F.J. (1987). P450 genes: structure, evolution, and regulation. Annu. Rev. Biochem. 56, 945–993.

Nelson, D.R., Kamataki, T., Waxman, D.J., Guengerich, F.P., Estabrook, R.W., Feyereisen, R., Gonzalez, F.J., Coon, M.J., Gunsalus, I.C., Gotoh, O., Okuda, K., and Nebert, D.W. (1993). The P450 superfamily: update on new sequences, gene mapping, accession numbers, early trivial names, and nomenclature. DNA 12, 1–51.

Pan, Z., Durst, F., Werck-Reichhardt, D., Gardner, H.W., Camara, B.,

Cornish, C., and Backhaus, R.A. (1995). The major protein of guayule rubber particles is a cytochrome P450. J. Biol. Chem. 270, 8487–8494.

Quail, P.H., Boylan, M.T., Parks, B.M., Short, T.W., Xu, Y., and Wagner, D. (1995). Phytochromes: photosensory perception and signal transduction. Science 268, 675–680.

Sambrook, J., Fritsch, E.F., and Maniatis, T. (1989). Molecular Cloning: A Laboratory Manual (Cold Spring Harbor, New York: Cold Spring Harbor Laboratory Press).

Takahashi, T., Gasch, A., Nishizawa, N., and Chua, N.-H. (1995). The DIMINUTO gene of Arabidopsis is involved in regulating cell elongation. Genes Dev. 9, 97–107.

Trezzini, G.F., Horrichs, A., and Somssich, I.E. (1993). Isolation of putative defense-related genes from Arabidopsis thaliana and expression in fungal elicitor-treated cells. Plant Mol. Biol. 21, 385–389.

Uknes, S., Mauch-Mani, B., Moyer, M., Potter, S., Williams, S., Dincher, S., Chandler, D., Slusarenko, A., Ward, E., and Ryals, J. (1992). Acquired resistance in Arabidopsis. Plant Cell 4, 645–656.

White, P.C., New, M.I., and Dupont, B. (1986). Structure of human steroid 21-hydroxylase genes. Proc. Natl. Acad. Sci. USA 83, 5111–5115.

Winkler, R.G., and Helentjaris, T. (1995). The maize Dwarf3 gene encodes a cytochrome P450-mediated early step in gibberellin biosynthesis. Plant Cell 7, 1307–1317.